Technical Report
RAL-TR-2001-014

CLRC

Calculated X-Ray Dichroic Signals and Resonant Bragg Diffraction Structure Factors for Dysprosium Borocarbide (DyB_2C_2)

S W Lovesey and K S Knight

26th February 2001

COUNCIL FOR THE CENTRAL LABORATORY OF THE RESEARCH COUNCILS

Enquiries about copyright, reproduction and requests for additional copies of this report should be addressed to:

The Central Laboratory of the Research Councils
Library and Information Services
Rutherford Appleton Laboratory
Chilton
Didcot
Oxfordshire
OX11 0QX
Tel: 01235 445384 Fax: 01235 446403
E-mail library@rl.ac.uk

ISSN 1358-6254

Calculated x-ray dichroic signals and resonant Bragg diffraction structure factors for dysprosium borocarbide (DyB_2C_2)

Stephen W. Lovesey and Kevin S. Knight

ISIS Facility, Rutherford Appleton Laboratory,
Oxfordshire OX11 0QX, England, UK.

Abstract

Low temperature properties of dysprosium borocarbide display evidence of two continuous phase transitions; it has been proposed that the first involves ordering of Dy quadrupole moments and, at a lower temperature, the second involves ordering of Dy magnetic moments. The latter has been established by magnetic neutron diffraction. Insight to the first phase transition, at T_Q, has been sought by resonant x-ray Bragg diffraction, which reveals charge-forbidden (Templeton-Templeton) intensities ($00l$ + ½) that increase continuously with decreasing temperature. We show that this scattering is absent if the space group is $P4/mbm$ which has been proposed for the high temperature crystal structure. Tanaka et al. (1999) report evidence that at T_Q the lattice distorts and the new space group is $P4_2/mnm$. The lower point-group symmetry of Dy ions in this space group is shown by us to allow diffraction at ($00l$ + ½) and, indeed, in part it is due to Dy quadrupole moments. In the magnetically ordered phase two neighbouring Dy moments along the c-axis are mutually perpendicular and two neighbouring moments in the plane normal to the c-axis are almost oppositely aligned. This magnetic configuration and point-group symmetry $2/m$ for Dy sites lead us to predict magnetic and charge scattering at reflections ($00l$ + ½) in the magnetically ordered phase. At reflections ($h0l$) and h odd calculated structure factors are purely magnetic. Our finding is consistent with data collected by Hirota et al. (2000) at the reflection (102). We report expressions for circular and linear dichroic signals and structure factors for Bragg scattering for the interpretation of future experiments. The structure factors are appropriate for azimuthal-angle scans in which the crystal is rotated about the ($00l$ + ½) or the ($h0l$) Bragg wavevectors.

PACS numbers: 75.25. +z, 61.10. – i, 75.10.Dg

1. Introduction

The tetragonal lanthanide compound DyB_2C_2 (dysprosium borocarbide) has properties consistent with a spontaneous spatial ordering of Dy quadrupole moments below T_Q = 24.7K. In the original investigation [1] antiferroquadrupole (AFQ) ordering was proposed in the interpretation of specific heat, magnetization and neutron diffraction measurements on a single crystal. The specific heat as a function of temperature shows two anomalies; one anomaly at T_c = 15.3K coincides with the onset of long-range magnetic order, established with neutron diffraction experiments, and the second at T_Q appears to have no magnetic content. A plausible model of features that set in at T_Q involves two nearly degenerate Kramers conjugate Dy states well separated in energy from the other 14 crystal-field states created from $^6H_{15/2}$. Orbital degrees of freedom in the doublet might contrive at T_Q to produce a phase transition and long-range ordering of 4f quadrupoles, with no accompanying magnetization anomaly, followed at T_c by ferromagnetic ordering of 4f magnetic moments.

Additional evidence for the development at T_Q of an AFQ configuration comes from the interpretation of x-ray diffraction data [2, 3, 4]. Indeed, it is believed that resonant x-ray Bragg diffraction near the Dy L_3 absorption edge can unambiguously answer the question as to whether or not an AFQ configuration arises in DyB_2C_2. To move beyond the current conjecture on this issue one needs a theoretical framework which links the observed diffraction pattern to 4f quadrupole moments.

In setting about building a suitable framework for the interpretation of resonant x-ray diffraction by a lanthanide compound one can sensibly start by creating the magnetic unit cell from individual ions, because a 4f valence shell is compact. The same starting point has been used to successfully interpret a wealth of other data on a wide range of compounds. In the future it will be possible to calculate structure factors, and other observable quantities, for lanthanide compounds from first principles as it is routinely done today for other compounds [5].

In the present study, each resonant ion is described by an atomic tensor $< T_m^{(K)} >$ where K is the rank, $-K \leq m \leq K$ and angular brackets denote the mean

value (equivalent to a thermadynamic average value) of the enclosed quantum mechanical operator [6]. The tensor of rank one contains the spin and orbital magnetic moments, and the tensor of rank two contains the quadrupole moment. In the absence of long-range magnetic order odd-rank tensors are zero.

Tensors for individual ions in the structure factor are related by symmetry elements derived from the chemical and magnetic structure. The symmetry elements create selection rules on K and m which depend on the Miller indices of a Bragg reflection, and the selection rules essentially specify the information to be found in a measurement. Evaluated for forward scattering the structure factor predicts the content of dichroic signals [7] which can be measured, for example, by fluorescence yield or absorption. In Bragg diffraction, reflections forbidden by the space group, also known as charge-forbidden reflections, reveal anisotropy in the valence shell [8, 9]. Their potential as valuable sources of information is more fully realized by performing azimuthal-angle scan in which the crystal is rotated about the Bragg wavevector.

In the next section we report the structure factor for the low temperature phase of DyB_2C_2. Input to the calculation includes the space group $P4_2/mnm$ proposed by Tanaka et al. [2] in order to index a superlattice peak (01 ½) that appears below T_Q. The authors attribute the superlattice peak to Thomson scattering associated with a lattice distortion which reduces the crystal symmetry from the space group $P4/mbm$ appropriate for temperatures in excess of T_Q. To the space group one adds the established magnetic structure, in which two neighbouring Dy moments along the c-axis are mutually perpendicular and two neighbouring moments in the plane normal to the c-axis are almost oppositely aligned. Calculated circular and linear dichroic signals at the Dy M_4 and M_5 absorption edges are reported in section 3. Structure factors that describe azimuthal-angle scans at charge-forbidden reflections are reported in sections 4 and 5. Our findings are gathered in section 6.

2. Chemical and magnetic structure

A projection normal to the c-axis of the chemical structure is shown in Fig. 1. Dichroic signals and resonant Bragg intensities are specific to resonant ions. In the

value (equivalent to a thermadynamic average value) of the enclosed quantum mechanical operator [6]. The tensor of rank one contains the spin and orbital magnetic moments, and the tensor of rank two contains the quadrupole moment. In the absence of long-range magnetic order odd-rank tensors are zero.

Tensors for individual ions in the structure factor are related by symmetry elements derived from the chemical and magnetic structure. The symmetry elements create selection rules on K and m which depend on the Miller indices of a Bragg reflection, and the selection rules essentially specify the information to be found in a measurement. Evaluated for forward scattering the structure factor predicts the content of dichroic signals [7] which can be measured, for example, by fluorescence yield or absorption. In Bragg diffraction, reflections forbidden by the space group, also known as charge-forbidden reflections, reveal anisotropy in the valence shell [8, 9]. Their potential as valuable sources of information is more fully realized by performing azimuthal-angle scan in which the crystal is rotated about the Bragg wavevector.

In the next section we report the structure factor for the low temperature phase of DyB_2C_2. Input to the calculation includes the space group $P4_2/mnm$ proposed by Tanaka et al. [2] in order to index a superlattice peak (01 ½) that appears below T_Q. The authors attribute the superlattice peak to Thomson scattering associated with a lattice distortion which reduces the crystal symmetry from the space group $P4/mbm$ appropriate for temperatures in excess of T_Q. To the space group one adds the established magnetic structure, in which two neighbouring Dy moments along the c-axis are mutually perpendicular and two neighbouring moments in the plane normal to the c-axis are almost oppositely aligned. Calculated circular and linear dichroic signals at the Dy M_4 and M_5 absorption edges are reported in section 3. Structure factors that describe azimuthal-angle scans at charge-forbidden reflections are reported in sections 4 and 5. Our findings are gathered in section 6.

2. Chemical and magnetic structure

A projection normal to the c-axis of the chemical structure is shown in Fig. 1. Dichroic signals and resonant Bragg intensities are specific to resonant ions. In the

space group 136 ($P4_2/mnm$) Dy ions are at sites 4 (c) with symmetry $2/m$ and the two-fold axis of rotation aligned with the c-axis. The four ions in the magnetic unit cell are at sites (0,0,0), (½a, ½b, 0), (0,0,½c) and (½a, ½b, ½c) and we label them 1, 2, 3 and 4, respectively, as in Fig. 2. In the construction of the structure factor the valence shell of a Dy ion is described by a spherical tensor $< T_m^{(K)}(j) >$ with j = 1, 2, 3 and 4. Ions 1 and 3 are related by a rotation of π/2 about the c-axis, and $< T_m^{(K)}(3) >= \exp(im\pi/2) < T_m^{(K)}(1) >$. A similar identity holds for ions 2 and 4. The ions 1 and 2 are related by reflection in a plane normal to the direction [½a, ½b, 0]. As for the spherical tensor this symmetry is equivalent to rotation by π about [½a, ½b, 0] because it is invariant with respect to inversion of the coordinates. A short calculation shows that such a rotation changes $< T_m^{(K)} >$ to $(-1)^K$ exp $(im\pi/2)$ $< T_{-m}^{(K)} >$. With respect to ion 1 the latter describes a ferromagnetic orientation. The required antiferromagnetic orientation, illustrated in Fig. 2, is brought about by reversing the polarity of the local field at site 2 and the operation introduces an additional phase factor $(-1)^K$. In this way we arrive at the identity $< T_m^{(K)}(2) >= \exp(im\pi/2) < T_{-m}^{(K)}(1) >$. The three identities we have derived allow the structure factor to be expressed in terms of $< T_m^{(K)}(1) >$ which we henceforth write without the site label j = 1.

It remains to discuss the influence on $< T_m^{(K)} >$ of the site symmetry $2/m$. Upon rotation by π about the c-axis $< T_m^{(K)} > \rightarrow \exp(im\pi) < T_m^{(K)} >$ and invariance with respect to the operation limits the projection label m to even integers. The full symmetry, however, is a union of site symmetry and magnetic symmetry, and consideration of the union shows that the aforementioned limit on the value of m is correct when the rank of the tensor is even. For K = 1 the atomic tensor behaves like orbital angular momentum. Rotation by π about the z-axis takes orthogonal coordinates (x, y, z) → (−x, −y, z). Under the same operation Cartesian components of orbital angular momentum (L_x, L_y, L_z) → ($-L_x$, $-L_y$, L_z), so the magnetic moment is also changed by the rotation. A union of rotation by π about the z-axis and reversal of the polarity of the local field, which is sometimes referred to as time reversal, changes (L_x, L_y, L_z) to (L_x, L_y, $-L_z$) and a moment confined to the x – y plane, meaning

$< L_z >= 0$, is invariant with respect to the combined operation. Such considerations applied to DyB_2C_2, with the Dy magnetic easy-axis in the plane normal to the crystal c-axis, lead to the selection rule $K + m$ = even integer, i.e. for $K = 1$ the allowed $m = \pm 1$.

3. Dichroic signals

Circular and linear dichroic signals are proportional to the structure factor evaluated for forward scattering. The quantity of interest is,

$$\begin{aligned} \Psi_m^{(K)} &= < T_m^{(K)}(1) > + < T_m^{(K)}(2) > + < T_m^{(K)}(3) > + < T_m^{(K)}(4) > \\ &= (1 + e^{im\pi/2})\{< T_m^{(K)} > + e^{im\pi/2} < T_{-m}^{(K)} >\}, \end{aligned} \tag{3.1}$$

where the second equality follows from identities established in the previous section. Contributions to $\Psi_m^{(K)}$ must satisfy the selection rule $K + m$ = even integer which is derived from the chemical and magnetic structure of DyB_2C_2.

The experiment is conveniently described in orthogonal axes formed from two states of polarization, labelled σ and π, and a unit vector $\hat{\mathbf{q}}$ in the direction of the beam of x-rays. The condition of the beam is described by a spherical tensor $X_m^{(K)}$, and the observed signal is related to the sum of scalar products [10],

$$\sum_K \mathbf{X}^{(K)} \cdot \mathbf{\Psi}^{(K)} = \sum_{K,m} (-1)^m X_{-m}^{(K)} \Psi_m^{(K)} . \tag{3.2}$$

This quantity is to be evaluated for different initial and final states of polarization; the four values are represented by $(\sigma\sigma)$, $(\sigma\pi)$, $(\pi\sigma)$ and $(\pi\pi)$. With this notation the circular dichroic signal is,

$$Z(\mathrm{C}) = \tfrac{i}{2} P_2 \{(\sigma\pi) - (\pi\sigma)\}, \tag{3.3}$$

where P_2 is the mean helicity of the x-ray beam. The parameter P_3 describes linear polarization along the σ– and π– axis; $P_3 = +1$ corresponds to complete polarization in the σ–direction and $P_3 = -1$ corresponds to complete polarization in the π–direction. (P_2 and P_3 are two of three components in the so-called Stokes vector [11].) The linear dichroic signal is,

$$Z(\mathrm{L}) = \tfrac{1}{2} P_3 \{(\sigma\sigma) - (\pi\pi)\}. \tag{3.4}$$

In the remaining part of this section we report values of Z(C) and Z(L) appropriate to absorption events which involve the Dy 3d core state and 4f valence shell, namely, electric dipole events at the Dy M_4 and M_5 absorption edges. First, though, we need to say more about crystal and principal axes.

The atomic tensor $< T_m^{(K)} >$ is defined with respect to crystal axes (a, b, c) illustrated in Fig. 2. Let these axes be related to the experimental axes $(\boldsymbol{\sigma}, \boldsymbol{\pi}, \hat{\mathbf{q}})$ by Euler angles α, β and γ [12]. For unit vectors directed along **a** and **c** one finds,

$$\hat{\mathbf{a}} = (\cos\alpha\cos\beta\cos\gamma - \sin\alpha\sin\gamma, \quad \sin\alpha\cos\beta\cos\gamma + \cos\alpha\sin\gamma, -\cos\gamma\sin\beta),$$

and (3.5)

$$\hat{\mathbf{c}} = (\cos\alpha\sin\beta, \quad \sin\alpha\sin\beta, \quad \cos\beta).$$

The physical properties of a Dy ion in Dy B_2C_2 illustrated in Fig. 2 are best described in terms of local principal axes (ξ, η, ζ); we choose to have ξ directed along the two-fold symmetry axis and ζ directed along the principal axis (cosϕ, sinϕ, 0) which is shown in Fig. 2. With this notation,

$$< T_m^{(K)} > = \sum_q D_{qm}^{(K)}(\phi, \tfrac{\pi}{2}, -\pi) < T_q^{(K)} >_{(\xi\eta\zeta)}, \tag{3.6}$$

where $D_{qm}^{(K)}$ is an element of the rotation matrix [12] and $< T_q^{(K)} >_{(\xi\eta\zeta)}$ is the Dy atomic tensor defined with respect to the principal axes. An electric dipole absorption event is described by a linear combination of atomic tensors of rank K = 0, 1 and 2 [10]. The tensors are subject to the selection rule $K + m$ even, and $m = \pm 2$ is not allowed by the structure factor (3.1).

The dichroic signals are different at the M_4 and M_5 absorption edges, characterized by total angular momentum $\bar{J} = 2 \pm \frac{1}{2}$. We find,

$$Z(\mathrm{C}) = \tfrac{1}{70} P_2 \sin\beta\cos\gamma \{(2\bar{J}+1) < L_\zeta > \pm 8 [< S_\zeta > + 3 < T_\zeta >]\}. \qquad (3.7)$$

In a J manifold of the 4f valence shell $< L_\zeta >$ and $< S_\zeta >$ are proportional to $< J_\zeta >$ and the Dy magnetic moment = (4/3) $< J_\zeta >$. The quantity $< T_\zeta >$ is less frequently encountered in magnetism [10]. It is a measure of magnetic anisotropy, and it is expected to be small compared to $< S_\zeta >$ which indeed is so with a saturated Dy ion; for the state with $< J_\zeta >$ = 15/2 and $< S_\zeta >$ = 5/2 we find $< T_\zeta >$ = – 1/3. The circular dichroic signal (3.7) vanishes for β = 0, which conforms to the established rule that the signal is proportional to the projection of the net moment on the direction of the x-ray beam [7]. With regard to the dependence of (3.7) on the Euler angle γ one should note that, with $\beta = \pi/2$ the angle γ measures the inclination of the net moment, directed along the a-axis, with respect to the direction of the beam. The atomic quantities in Z(C) are zero in the absence of long-range magnetic order, and for DyB_2C_2 the signal is expected to develop as the temperature is lowered through T_c.

Turning to the linear dichroic signal, calculated from (3.4), we encounter quite different atomic quantities to those in (3.7). First, there is the quadrupole moment $< \mathbf{Q} >$ which is due solely to orbital angular momentum. By measuring at both the M_4 and M_5 edges one can find values for two other atomic quantities, denoted by <**P**> and <**R**>, which are related to spin and orbital angular momentum [10]. In giving the result for Z(L) it is convenient to use, for example,

$$< A_{\xi\eta} > = < A_{\eta\xi} > = -\frac{1}{350}\{(2\bar{J}+1) < Q_{\xi\eta} > \pm \frac{4}{5}[10 < P_{\xi\eta} > +3 < R_{\xi\eta} >]\}. \quad (3.8)$$

The linear dichroic signal contains in addition to $<A_{\xi\eta}>$ the atomic quantities $<A_{\xi\xi}>$, $<A_{\eta\eta}>$ and $<A_{\zeta\zeta}>$ and these are defined in accord with (3.8) on using the appropriate Cartesian labels.

We find,

$$Z(\mathrm{L}) = P_3 \cos 2\alpha \sin^2 \beta\{- < A_{\zeta\zeta} > + < A_{\xi\xi} - A_{\eta\eta} > \cos 2\phi + 2 < A_{\xi\eta} > \sin 2\phi\}. \quad (3.9)$$

If the signal is summed over the two partners of the 3d absorption edge, labelled by $\bar{J} = 3/2(M_4)$ and $\bar{J} = 5/2(M_5)$, there is a direct measure of a linear combination of three components of the quadrupole moment. Unlike Z(C), we find that Z(L) depends explicitly on the canting angle ϕ. The geometric factor cos2α in (3.9) is a signature of linear dichroism unrelated to the point-group symmetry of the site occupied by the resonant ion. In the case of DyB_2C_2, an AFQ configuration setting in below T_Q could lead to a strong dependence of Z(L) on temperature. By way of orientation to the magnitude of atomic quantities in Z(L) we give their values for a saturated Dy ion. In this instance, there is one component, $<A_{\zeta\zeta}>$, different from zero and $<Q_{\zeta\zeta}> = -15/2$, $<P_{\zeta\zeta}> = 5/2$ and $<R_{\zeta\zeta}> = 0$.

4. Bragg diffraction at $(00l + ½)$

Our interest here is Bragg diffraction at charge-forbidden reflections $(00l + ½)$ and l is an integer. In the absence of long-range magnetic order one observes Templeton-Templeton scattering [8, 9], which is a good probe of spatial anisotropy. To this end it is usual to execute azimuthal-angle scans in which the crystal is rotated about the Bragg wavevector and two such studies of DyB_2C_2 have been reported [2, 4].

The structure factor for diffraction at $(00l + ½)$ is proportional to,

$$\begin{aligned}\Psi_m^{(K)} &= < T_m^{(K)}(1) > + < T_m^{(K)}(2) > - < T_m^{(K)}(3) > - < T_m^{(K)}(4) > \\ &= \{1 - e^{im\pi/2}\}\{< T_m^{(K)} > + e^{im\pi/2} < T_{-m}^{(K)} >\},\end{aligned} \tag{4.1}$$

and $K + m$ is an even integer. Evidently with K even, which accounts for Templeton-Templeton scattering, the allowed values of m are ± 2. These values of the projection label are consistent with the point-group symmetry $2/m$ of Dy in the space group 136 which allows $m = 0, \pm 2$. Above the temperature T_Q the structure of DyB_2C_2 belongs to the space group 127; in this space group the point-group symmetry of Dy sites is $4/m$ which allows $m = 0, \pm 4$, and according to (4.1) both these values give null scattering at $(00l + ½)$. One concludes that a distortion of the structure at T_Q, which lowers the crystal symmetry from one in which the Dy site symmetry is $4/m$ to one in which it is $2/m$, is capable of producing both the superlattice peak $(01½)$ and the Templeton-Templeton scattering at (003/2) which has been observed by Tanaka et al. [2].

An electric quadrupole (E2) event at the Dy 2p absorption edge gives direct access to the 4f valence shell. The reported energy dependence at the L_3 absorption edge of the integrated intensity for $(00l + ½)$ shows a pre-edge feature which is most likely due to an E2 event. The associated structure factor is derived from $\Psi_m^{(K)}$ in (4.1) by much the same algebra encountered in calculating dichroic signals from (3.1) and (3.2) [13]. In place of $\mathbf{X}^{(K)}$ in (3.2) we have for an E2 event a spherical tensor that

depends on the direction and polarization of both the primary and secondary x-ray beams. In diffraction the primary beam is deflected through an angle 2θ, and an azimuthal-angle scan is rotation of the crystal by ψ about the Bragg wavevector.

The standard experimental geometry is one in which σ-polarization is perpendicular to the plane of scattering. Orthogonal right-handed axes (x, y, z) are defined as follows; the x-axis is in the opposite direction to the Bragg wavevector $(00l + ½)$ and the z-axis is parallel to σ-polarization. For $\psi = 0$ the crystal axes (a, b, c) in the experimental geometry are (–c, –a, b), i.e. the origin of an azimuthal-angle scan has the crystal a-axis in the plane of scattering and during a scan the plane containing Dy principal axes is normal to the plane of scattering.

The structure factors are chosen to be dimensionless. In this respect they differ from previous results for saturated lanthanide ions [13]; the scale factor between the two calculations is,

$$\frac{6}{(35)^{3/2}}\{q < \mathrm{np} \mid R^2 \mid 4\mathrm{f} >\}^2.$$

On going from $L_{2,3}$ to $M_{2,3}$ absorption edges the magnitude of the electric quadrupole matrix element $<\mathrm{np}|R^2|4\mathrm{f}>$ increases by at least an order of magnitude.

The four structure factors are denoted by $F_{\sigma'\sigma}$, $F_{\sigma'\pi}$, $F_{\pi'\sigma}$, and $F_{\pi'\pi}$. We find $F_{\sigma'\pi} = - F_{\pi'\sigma}$. In the results, tensors of even rank which arise are $< T^{(2)}_{+2} >$ and $< T^{(4)}_{+2} >$. It is useful to note that [12],

$$< T^{(2)}_{+2} >= \frac{1}{\sqrt{6}} < T^{(2)}_{aa} - T^{(2)}_{bb} + 2\mathrm{i}\, T^{(2)}_{ab} >, \tag{4.2}$$

and in the principal axes the corresponding tensor is,

$$< T^{(2)}_{+1} >_{(\xi\eta\zeta)} = -(\tfrac{2}{3})^{1/2} < T^{(2)}_{\xi\zeta} + \mathrm{i}\, T^{(2)}_{\eta\zeta} > . \tag{4.3}$$

The quantities entering the structure factors are,

$$\mathrm{Im.}<T^{(2)}_{+2}> = \mathrm{Im.}\{e^{-i\phi}<T^{(2)}_{+1}>_{(\xi\eta\zeta)}\}, \tag{4.4}$$

and,

$$\mathrm{Im.}<T^{(4)}_{+2}> = \frac{1}{2\sqrt{2}}\,\mathrm{Im.}\{-e^{-i\phi}<T^{(4)}_{+1}>_{(\xi\eta\zeta)} + \sqrt{7}\,e^{-3i\phi}<T^{(4)}_{+3}>_{(\xi\eta\zeta)}\}, \tag{4.5}$$

where ϕ is the angled enclosed by the Dy principal axis and the crystal a-axis. These expressions make clear that, in the absence of long-range magnetic order, scattering is due to anisotropy in the 4f valence shell. Tensors of odd-rank in the structure factors are obtained from (3.6) with $q = 0$ and this is consistent with Dy magnetic moments normal to the crystal c-axis.

Our results for the three structure factors are:

$$\begin{aligned} F_{\sigma'\sigma} &= \sin(2\psi)\sin^2\theta\,\mathrm{Im.}\{3\sqrt{2}<T^{(2)}_{+2}> - \sqrt{11}<T^{(4)}_{+2}>\} \\ &+ i\delta\cos\psi\sin(2\theta)\{-2\sqrt{2}<T^{(1)}_{0}>_{(\xi\eta\zeta)} + 3<T^{(3)}_{0}>_{(\xi\eta\zeta)}(5\cos^2\psi - 3)\}, \end{aligned} \tag{4.6}$$

$$\begin{aligned} F_{\pi'\pi} &= \sin(2\psi)\,\mathrm{Im.}\{3\sqrt{2}<T^{(2)}_{+2}>\cos 4\theta - \tfrac{1}{8}\sqrt{11}<T^{(4)}_{+2}>(7+\cos 4\theta)\} \\ &- \tfrac{i}{2}\delta\cos\psi\sin(4\theta)\{8\sqrt{2}<T^{(1)}_{0}>_{(\xi\eta\zeta)} + 3<T^{(3)}_{0}>_{(\xi\eta\zeta)}(5\cos^2\psi - 3)\}, \end{aligned} \tag{4.7}$$

and

$$\begin{aligned} F_{\pi'\sigma} &= -\cos(2\psi)\sin\theta\,\mathrm{Im.}\{3\sqrt{2}<T^{(2)}_{+2}>(3-4\sin^2\theta) + \tfrac{1}{2}\sqrt{11}<T^{(4)}_{+2}> \\ &(1+\sin^2\theta)\} - i\delta\sin\psi\cos\theta\{2\sqrt{2}<T^{(1)}_{0}>_{(\xi\eta\zeta)}(3-4\cos^2\theta) \\ &+ 3<T^{(3)}_{0}>_{(\xi\eta\zeta)}(9-12\cos^2\theta - 10\sin^2\psi + 15\cos^2\theta\sin^2\psi)\}. \end{aligned} \tag{4.8}$$

In these results $\delta = 7/4\sqrt{30}$. When the primary x-ray beam is linearly polarized diffracted intensities are proportional to $|F|^2$ and there is no interference between even-rank (charge) and odd-rank (magnetic) spherical tensors.

Above the magnetic critical temperature T_c odd-rank tensors are zero. The structure factors are purely real and as a function of azimuthal angle Bragg intensities are four-fold periodic. Rotated and unrotated channels of scattering are out of phase and there is no scattering in the unrotated channels at the origin of the azimuthal-angle scan. We find the same dependence on the azimuthal angle with E1 and E2 enhanced diffraction, and our results for E1 agree with results obtained by Tanaka et al. [2]. Our findings apply to DyB_2C_2 in the temperature interval $T_c \leq T \leq T_Q$ and they agree with observations [2, 4].

Contributions from even-rank and odd-rank tensors are 90° out of phase. This feature is expected and it means scattering by the magnetically ordered phase of DyB_2C_2 is sensitive to circular polarization. Bragg intensities contain an interference between charge and magnetic amplitudes, induced by circular polarization in the primary beam, which is proportional to,

$$P_2 \, \mathrm{Im.}\{F^*_{\pi'\pi} F_{\pi'\sigma} - F_{\sigma'\sigma} F^*_{\pi'\sigma}\},$$

where P_2 is the helicity of the primary beam. If the primary beam is purely σ-polarized (P_3=1) the diffracted beam carries circular polarization proportional to $\mathrm{Im.}\{F_{\sigma'\sigma} F^*_{\pi'\sigma}\}$. Of course, both interference effects vanish on raising the temperature of the sample through T_c.

With regard to azimuthal-angle scans the ψ-dependence of the intensity of pure magnetic scattering is two-fold periodic, and the origin is shifted by π/2 with respect to pure charge scattering. In the unrotated channels magnetic scattering vanishes for $\psi = \pi/2$ which corresponds to the net moment, directed along the crystal a-axis, normal to the plane of scattering. The rotated amplitude is proportional to sinψ and the associated intensity vanishes when the net amount lies in the plane of scattering.

The dependence of the magnetic amplitudes on ψ is different at charge-forbidden and change-allowed reflections. Structure factors calculated with (3.1) and (4.1) have magnetic components shifted by $\pi/2$ in ψ, and results derived from (3.1) are entirely consistent with previous findings for saturated lanthanide ions [13].

In principle, atomic quantities in the structure factors can be calculated. To this end one needs a model of the Dy ions which includes interactions that cause the pronounced change in intensity with temperature. As we saw in the previous section, tensors of rank one and rank two contain familiar atomic quantities. For the p $\rightarrow$f (E2) absorption event under discussion here one finds ($\bar{J} = 1 \pm \frac{1}{2}$),

$$< \mathbf{T}^{(1)} >= \frac{1}{12\sqrt{21}} \{(2\bar{J}+1) < \mathbf{L} > \pm 4[< \mathbf{S} > +3 < \mathbf{T} >]\}, \qquad (4.9)$$

and,

$$< \mathbf{T}^{(2)} >= \frac{1}{18\sqrt{105}} \{(2\bar{J}+1) < \mathbf{Q} > \pm \frac{2}{5} [10 < \mathbf{P} > +3 < \mathbf{R} >]\}. \qquad (4.10)$$

Here, <**L**>, <**S**> and <**Q**> are the orbital, spin and quadrupole moments of the Dy 4f valence shell, and the remaining three atomic quantities in (4.9) and (4.10) arise also in section 3 in the interpretation of dichroic signals. For the extreme model of a saturated Dy ion there is no (Templeton-Templeton) charge scattering at the reflection (00l + ½) because all tensors are diagonal, i.e. $< T_m^{(K)} > = 0$ for $m \neq 0$, and for magnetic amplitudes one finds,

$$< T_0^{(1)} >= \frac{5}{12\sqrt{21}} \{(2\bar{J}+1) \pm \frac{6}{5}\}, \quad \text{and} \quad < T_0^{(3)} >= \pm \frac{1}{9} (\frac{1}{42})^{1/2}.$$

5. Bragg diffraction at (*h*0*l*) and *h* odd

Charge-forbidden reflections (*h*0*l*) and *h* odd are purely magnetic. This finding follows directly from,

$$\Psi_m^{(K)} = < T_m^{(K)}(1) > - < T_m^{(K)}(2) > + < T_m^{(K)}(3) > - < T_m^{(K)}(4) >$$
$$= \{1 + e^{im\pi/2}\}\{< T_m^{(K)} > - e^{im\pi/2} < T_{-m}^{(K)} >\}, \tag{5.1}$$

which vanishes for $m = 0$ and $m = \pm 2$, the values of m allowed by the point-group $2/m$. For DyB_2C_2 one has the selection rule $K + m$ even. We reach the conclusion that at (*h*0*l*) and *h* odd there is no scattering caused by even-rank (charge) spherical tensors. Our finding is consistent with observations at (102) reported in [4], which shows a Bragg intensity as a function of temperature constant in the region $T_c \leq T \leq T_Q$ and below T_c the intensity continuously increases with decreasing temperature.

Below T_c the Bragg intensity is described by structure factors calculated from (5.1) and the terms $K = 1$ and 3. The origin of the azimuthal-angle scan $\psi = 0$ has the crystal b-axis perpendicular to the plane of scattering, and aligned with σ-polarization. We find that the structure factors are the same, apart from a sign, as the magnetic content of equations (4.6) and (4.7), namely, on keeping only that part of (4.6) and (4.7) which contains δ one has $F_{\sigma'\sigma}$ (*h*0*l*) = – equation (4.6) and $F_{\pi'\sigma}$ (*h*0*l*) = equation (4.7).

6. Discussion

We have demonstrated that the space group $P4_2/mnm$ and point-group symmetry $2/m$ for Dy sites is consistent with Templeton and Templeton scattering observed in experiments on DyB_2C_2 [2, 4]. The scattering in question, observed at reflections $(00l + ½)$, appears as the sample temperature falls below $T_Q = 24.7$K and at this temperature the specific heat shows an anomaly with no magnetic content [1]. The calculated structure factors, for rotated and unrotated states of polarization, show

that the scattering amplitude is a linear combination of spherical tensors, of ranks two and four, which includes the Dy 4f quadrupole moment. Our result for the linear dichroic signal reveals that an appropriate experiment is a direct measure of the quadrupole moment.

The configuration of magnetic moments assumed in our calculation is consistent with neutron diffraction data [1]. On this basis, and point-group symmetry $2/m$ for Dy sites, we show that magnetic and charge diffraction contribute below the magnetic critical temperature to the reflection $(00l + ½)$. Charge and magnetic amplitudes do not depend in the same way on the azimuthal-angle ψ which measures rotation of the crystal about the $(00l + ½)$ Bragg wavevector. Interference of the two amplitudes is brought about by circular polarization in the primary beam. In the diffracted beam the concomitant effect is creation of circular polarization from a primary beam which is purely linearly polarized. Both effects, involving circular polarization, vanish on loss of long-range magnetic order.

At the reflection $(h0l)$ and h odd we find the calculated intensity is purely magnetic. This result is consistent with data at (102) reported by Hirota et al. [4]. The intensity observed at (102) is independent of temperature down to the magnetic critical temperature and below T_c the intensity continuously increases with decreasing temperature.

Acknowledgements

We are grateful to Dr. Y. Tanaka for several discussions about x-ray scattering by dysprosium borocarbide, and for letting us have sight of unpublished experimental data. Dr. U. Staub supplied us with crystal-field calculations appropriate for site symmetry $2/m$.

Fig. 1

The c-axis of the crystal DyB_2C_2 is normal to the plane of the diagram. The buckling of B and C rings of ions sets in at the temperature $T_Q = 24.7K$ and it reduces the point-group of sites occupied by Dy ions to $2/m$, from $4/m$ in the space group $P4/mbm$ which is appropriate at high temperatures.

Fig. 2

The diagram illustrates the sites and magnetic configuration of the four Dy ions in the magnetic unit cell. The principal axis of the Dy ion labelled 1 lies in the a-b plane, which is normal to the two-fold axis of rotational symmetry, and it subtends an angle ϕ with the a-axis, namely, it is the vector $(\cos\phi, \sin\phi, 0)$. Principal axes of Dy ions 2, 3 and 4, respectively, are $(-\sin\phi,-\cos\phi, 0)$, $(-\sin\phi,\cos\phi, 0)$ and $(\cos\phi, -\sin\phi, 0)$. Below T_c the net moment is directed along the a-axis and it vanishes should $\phi = 45°$.

References:

[1] Yamauchi H et al. 1999 J. Phys. Soc. Jpn. **68** 2057

[2] Tanaka Y et al. 1999 J. Phys.: Condens. Matter **11** L505

[3] Tanaka Y, private communication

[4] Hirota K et al. 2000 Phys. Rev. Lett. **84** 2706

[5] Strange P et al. 1999 Letter to Nature **399** 756.

[6] Carra P and Thole BT 1994 Rev. Mod. Phys. **66** 1509

[7] Thole BT, Carra P, Sette F and van der Laan G 1992 Phys. Rev. Lett. **68** 1943, and van der Laan G 1994 J.Phys.Soc. Jpn. **63** 2393.

[8] Templeton D H and Templeton L K 1994 Phys. Rev. **B49** 14850

[9] Templeton D H, Acta Cryst. 1998 **A54** 158

[10] Lovesey SW and Balcar E 1997 J. Phys. : Condens. Matter **9** 4237 – ibid **9** 8679

[11] Berestetskii VB, Lifshitz EM and Pitaevskii LP 1982 Quantum Electrodynamics (Oxford : Pergamon Press)

[12] Varshalovich DA, Moskalev AN and Khersonakii VK 1988 Quantum Theory of Angular Momentum (Singapore: World Scientific)

[13] Lovesey SW, Fritz O and Balcar E 1998 J. Phys. : Condens. Matter **10** 501

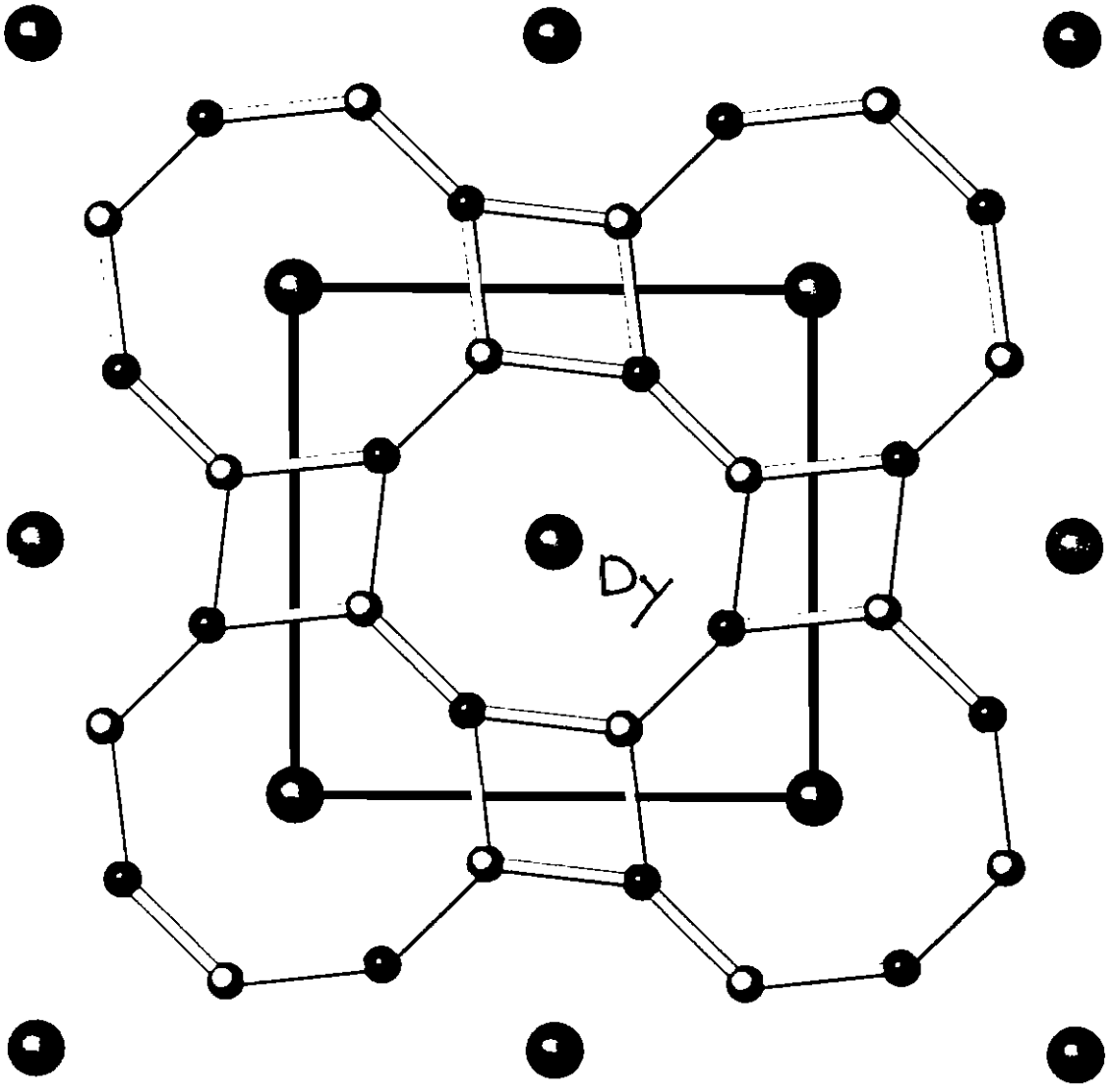

Fig. 1

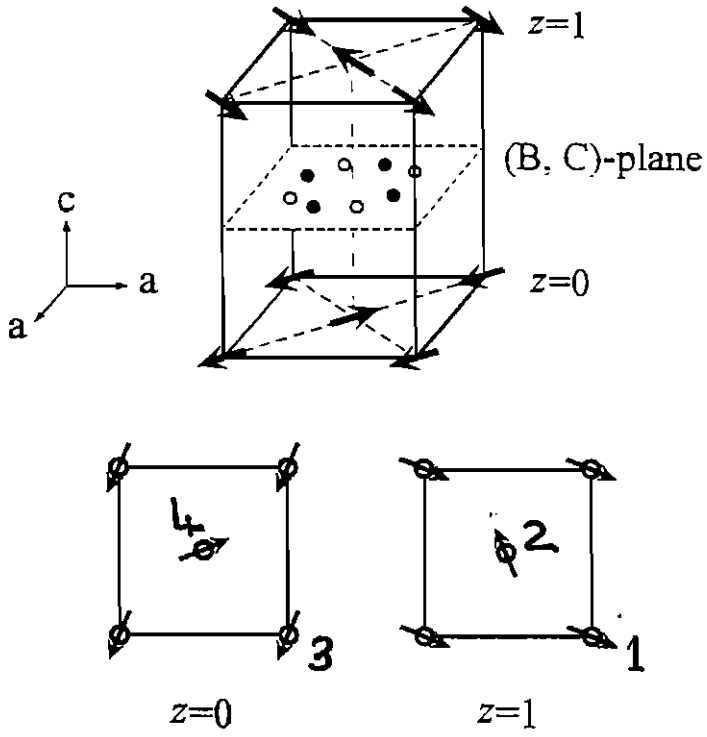

Fig. 2.